Supporting Information: Mesoporous Multi-Valence Manganese Oxides Composite Nanotubes Boosting Long-Life Lithium-Ion Batteries

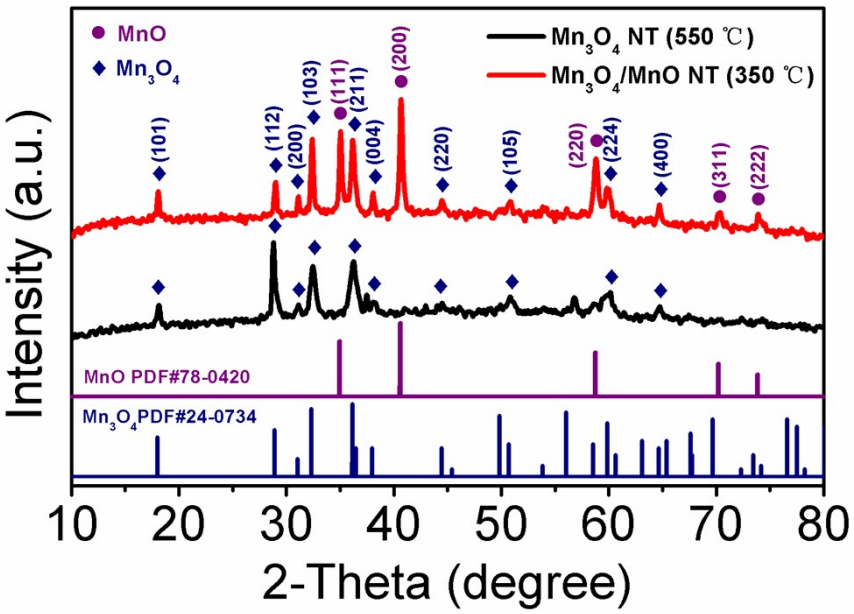

Fig.S1 XRD patterns for Reference group (β-MnO_2 nanotubes with C-coating) annealing at 300 ℃ and 500 ℃.

Tab.S1 Comparison of the actual crystalline phase of experimental group and reference group.

Annealing temperature		**Room**	**300℃**	**500 ℃**
Experimental	Subjects	β-MnO_2 NT	β-MnO_2 NT@PDA	β-MnO_2 NT@PDA
group	Crystalline phase	β-MnO_2	β-MnO_2/Mn_3O_4@C	Mn_3O_4@C
Reference	Subjects	β-MnO_2 NT	β-MnO_2 NT	β-MnO_2 NT
group	Crystalline phase	β-MnO_2	Mn_3O_4	Mn_3O_4/MnO

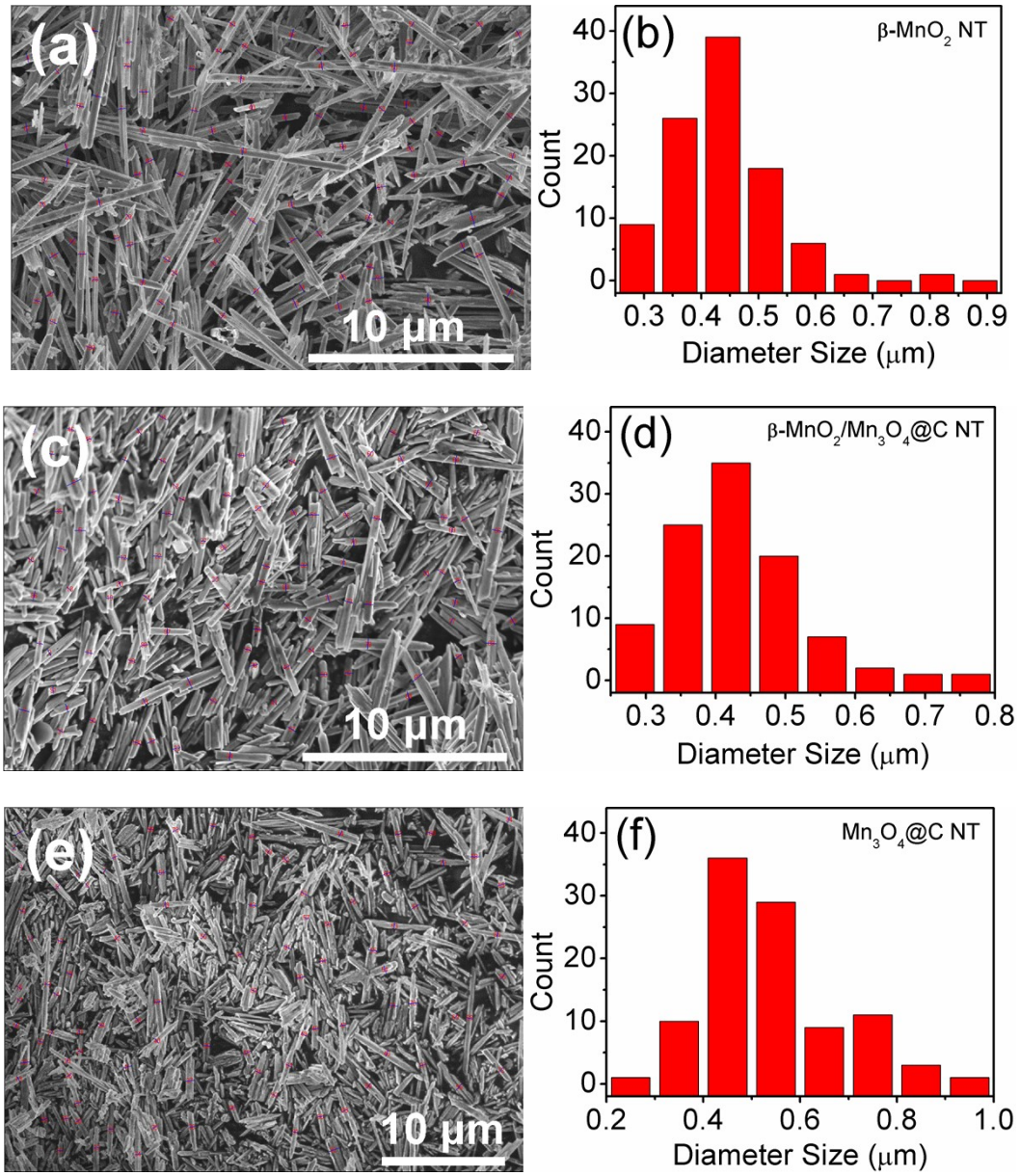

Fig.S2 SEM image sampling and diameter frequency distribution for (a) and (b) β-MnO_2 NT, (c) and (d) β-MnO_2/Mn_3O_4@C NT, (e) and (f) Mn_3O_4@C NT.

Tab.S2 The average diameter of all manganese oxide nanotubes obtained from Fig.S4.

Sample	**Average Diameter （nm）**
β-MnO_2 NT	~440
β-MnO_2/Mn_3O_4@C NT	~420
Mn_3O_4@C NT	~450

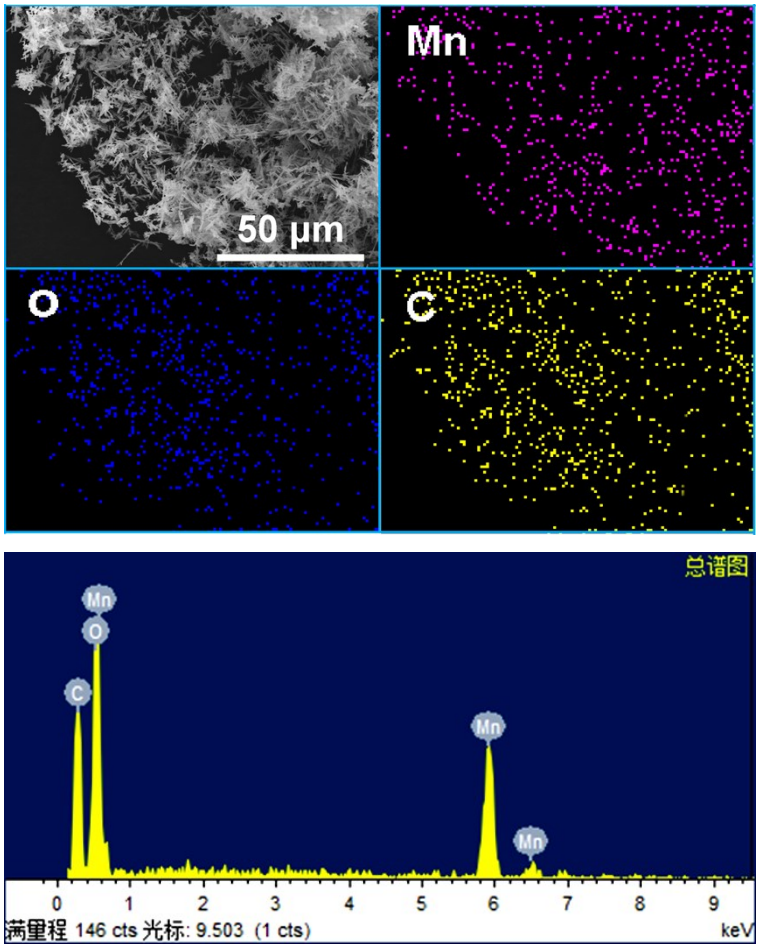

Fig.S3 The EDS patterns of the β-MnO_2/Mn_3O_4@C NT and its EDS elemental mappings.

Tab.S3 According to the same equivalent circuit model, calculated Rs, Rct and C for β-MnO_2 NT, Mn_3O_4@C NT, and β-MnO_2/Mn_3O_4@C NT at initial, respectively.

Sample	**initial**		
	Rs (Ohm)	**Rct (Ohm)**	**C (F)**
β-MnO_2 NT	2.406	501.000	0.00327
β-MnO_2/Mn_3O_4@C NT	4.676	365.100	0.00652
Mn_3O_4@C NT	2.570	301.000	0.00278

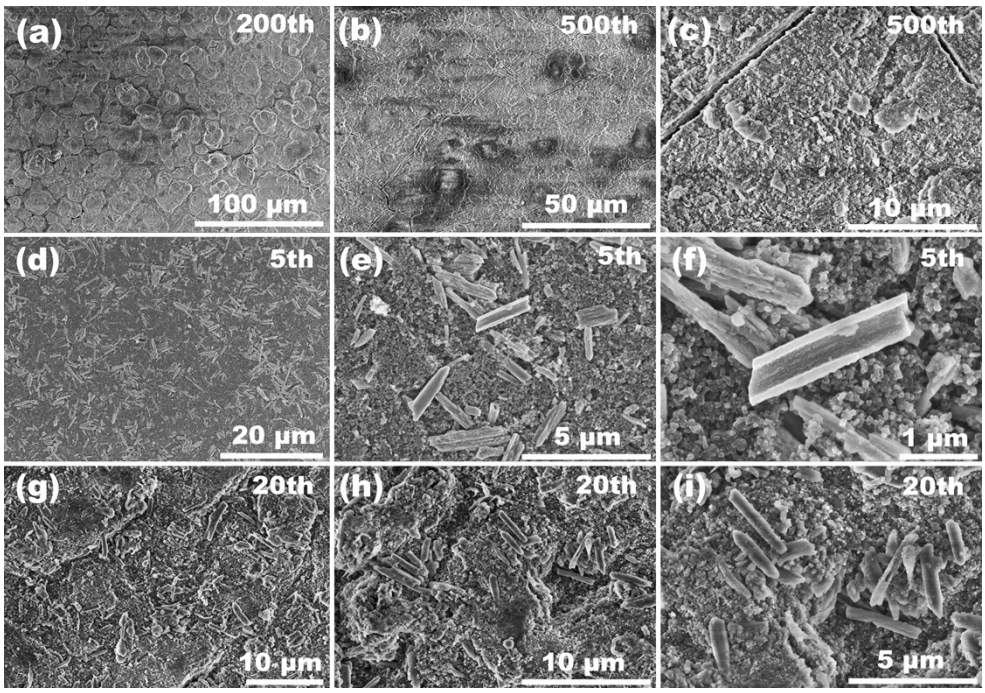

Fig.S4 During the charge and discharge cycle, SEM images for (a)-(c) Mn_3O_4@C NT, (d)-(i) SEM images for β-MnO_2/Mn_3O_4@C NT.

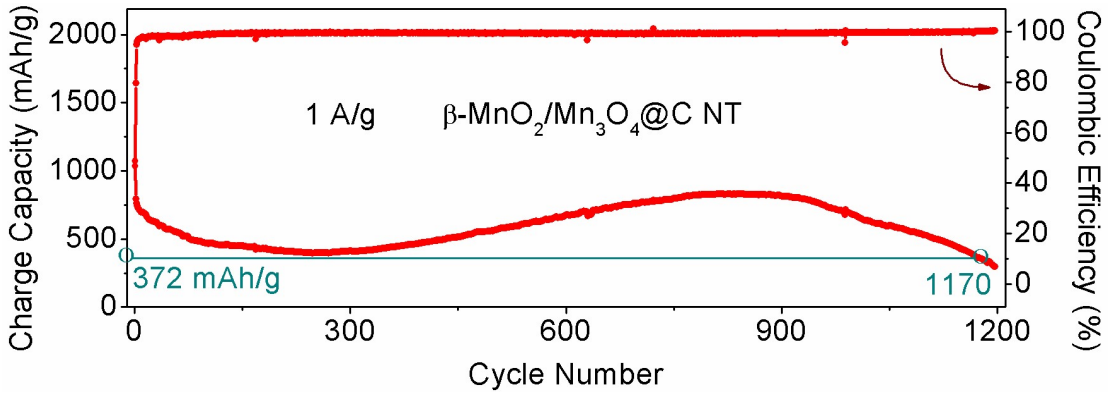

Fig.S5 The cycle property for β-MnO_2/Mn_3O_4@C NT at 1 A g^{-1}.

Tab.S4 Electrochemical performance of β-MnO_2/Mn_3O_4@C NT electrodes in this work, compared with some other manganese oxides (eg. MnO, MnO_2, Mn_2O_3, and Mn_3O_4 etc.) electrodes reported in previous literature.

Binder	Type of materials	Initial charge capacity	Cycle stability (1C = 936 mA g^{-1})
use	This work	1137 mAh g^{-1} at 0.2 A g^{-1}	679 mAh g^{-1} after 1000 cycles at 1 A g^{-1}
free	Porous Mn_3O_4 nanosheets@3D-Cu[1]	1166 mAh g^{-1} at 0.2 A g^{-1}	668 mAh g^{-1} after 1005 cycles at 1 A g^{-1}
use	$MnCO_3$/Mn_3O_4/RGO composites[2]	828 mAh g^{-1} at 0.1 A g^{-1}	532 mAh g^{-1} after 800 cycles at 1 A g^{-1}

use	Hollow Mn_2O_3 Core-shell Microspheres[3]	935 mAh g^{-1} at 0.1 A g^{-1}	620 mAh g^{-1} after 500 cycles at 1 A g^{-1}
use	MOFs-derived Porous Mn_2O_3[4]	852 mAh g^{-1} at 0.5 A g^{-1}	705 mAh g^{-1} after 250 cycles at 1 A g^{-1}
use	Porous MnO/C nanotubes[5]	810 mAh g^{-1} at 0.1 A g^{-1}	618 mAh g^{-1} after 200 cycles at 0.5 A g^{-1}
use	CNTs-entangled Mn_3O_4 octahedrons[6]	780 mAh g^{-1} at 0.19 A g^{-1}	678 mAh g^{-1} after 400 cycles at 0.468 A g^{-1}
use	MnO_2 nanoflakes@carbon nanohorns[7]	785 mAh g^{-1} at 0.1 A g^{-1}	552 mAh g^{-1} after 50 cycles at 0.45 A g^{-1}
free	Porous MnO nanoflakes@Ni foam[8]	570 mAh g^{-1} at 0.25 A g^{-1}	569 mAh g^{-1} after 100 cycles at 0.25 A g^{-1}
use	Mesoporous Mn_2O_3/RGO composites[9]	931 mAh g^{-1} at 0.2 A g^{-1}	1015 mAh g^{-1} after 130 cycles at 0.23 A g^{-1}
use	Nanoflaky MnO_2@carbon nanotubes[10]	805 mAh g^{-1} at 0.2 A g^{-1}	620 mAh g^{-1} after 50 cycles at 0.2 A g^{-1}
use	MnO_2/3D porous graphene composites[11]	927 mAh g^{-1} at 0.1A g^{-1}	836 mAh g^{-1} after 200 cycles at 0.1 A g^{-1}
sue	N-Doped MnO/Graphene Nanosheets[12]	829 mAh g^{-1} at 0.05 A g^{-1}	772 mAh g^{-1} after 90 cycles at 0.1 A g^{-1}
use	Mn_3O_4 @RGO nanowires[13]	802 mAh g^{-1} at 0.1 A g^{-1}	702 mAh g^{-1} after 100 cycles at 0.1 A g^{-1}
free	Mn_2O_3 nanowires@Ti foil[14]	498 mAh g^{-1} at 0.1 A g^{-1}	502 mAh g^{-1} after 100 cycles at 0.1 A g^{-1}

* Compared with some other manganese oxides (eg. MnO, MnO_2, Mn_2O_3, and Mn_3O_4 etc.), it is clearly seen that the β-MnO_2/Mn_3O_4@C NT electrodes in this work exhibits the best property, particularly the cycle property at a high current density of 1 A g^{-1}.

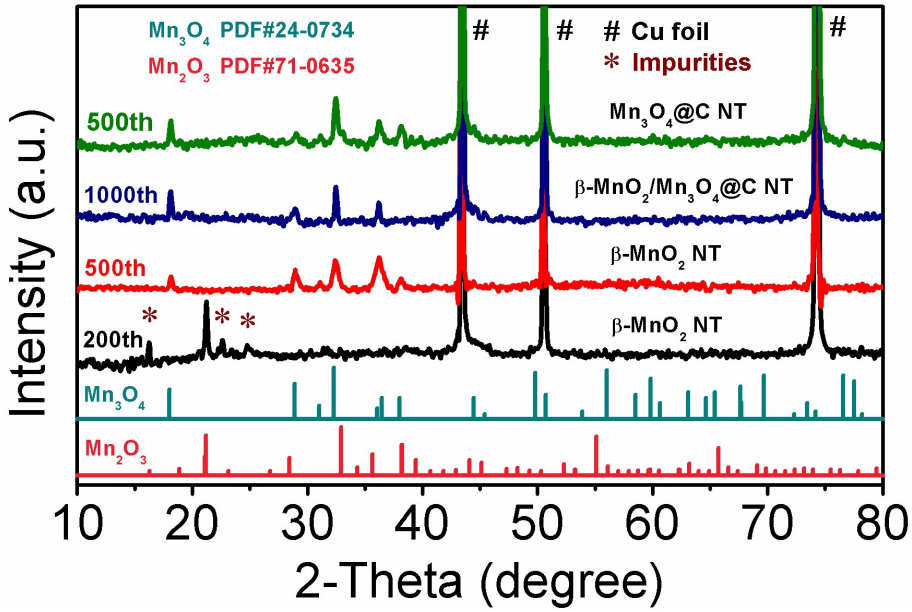

Fig.S7 XRD patterns for three electrode materials for β-MnO_2 NT, β-MnO_2/Mn_3O_4@C NT, and Mn_3O_4@C NT in different stages of the cycle under 1 A g^{-1}, respectively.

Tab.S5 The actual phase structure of the three electrode materials for β-MnO_2 NT, β-MnO_2/Mn_3O_4@C NT, and Mn_3O_4@C NT in different stages of the cycle under 1 A g^{-1} obtained from Fig.S9 and Fig. 2.

Cycle number	β-MnO_2 NT	β-MnO_2/Mn_3O_4@C NT	Mn_3O_4@C NT
initial phase	β-MnO_2	β-MnO_2/Mn_3O_4	Mn_3O_4
200th phase	Mn_2O_3	——	——
500th phase	Mn_3O_4	——	——
800th phase	——	——	Mn_3O_4
1000th phase	——	Mn_3O_4	——

* Because it takes much time to monitor the cycle process, it is very difficult. In order to reduce the workload, only limited nodes are selected for testing, but this does not affect the conclusion of the experiment.

Reference

[1] X.-Y. Fan, Y. Cui, P. Liu, L. Gou, L. Xu, D.-L. Li, PCCP 2016, 18, 22224.

[2] R. Zhang, D. Wang, L. C. Qin, G. W. Wen, H. Pan, Y. F. Zhang, N. Tian, Y. Zhou, X. Huang, J. Mater. Chem. A 2017, 5.

[3] C. Zhang, C. Guo, Y. Wei, L. Hou, Phys. Chem. Chem. Phys. 2016, 18, 4739.

[4] Z. Bai, Y. Zhang, Y. Zhang, C. Guo, B. Tang, D. Sun, J. Mater. Chem. A 2015, 3, 5266.

[5] G. L. Xu, Y. F. Xu, H. Sun, F. Fu, X. M. Zheng, L. Huang, J. T. Li, S. H. Yang, S. G. Sun, Chem. Commun. 2012, 48, 8502.

[6] X. Cui, Y. Wang, Q. Xu, P. Sun, X. Wang, T. Wei, Y. Sun, Nanotechnology 2017, 28, 255402.

[7] H. Lai, J. Li, Z. Chen, Z. Huang, ACS Appl Mater Interfaces 2012, 4, 2325.

[8] X. Li, D. Li, L. Qiao, X. Wang, X. Sun, P. Wang, D. He, J. Mater. Chem. 2012, 22.

[9] H. S. Jadhav, G. M. Thorat, B. B. Kale, J. G. Seo, Dalton Trans 2017, 46, 9777.

[10] H. Xia, M. O. Lai, L. Lu, J. Mater. Chem. 2010, 20, 6896.

[11] Y. Li, Q. Zhang, J. Zhu, X. L. Wei, P. K. Shen, J. Mater. Chem. A 2014, 2, 3163.

[12] K. Zhang, P. Han, L. Gu, L. Zhang, Z. Liu, Q. Kong, C. Zhang, S. Dong, Z. Zhang, J. Yao, H. Xu, G. Cui, L. Chen, ACS Appl Mater Interfaces 2012, 4, 658.

[13] J. G. Wang, D. Jin, R. Zhou, X. Li, X. R. Liu, C. Shen, K. Xie, B. Li, F. Kang, B. Wei, Acs Nano 2016, 10, 6227.

[14] Y. Wang, Y. Wang, D. Jia, Z. Peng, Y. Xia, G. Zheng, Nano Lett. 2014, 14, 1080.